



Breakdown of magnetic order in Mott insulators with frustrated superexchange interaction

J.-S. Zhou,^{1,2,*} Y. Uwatoko,¹ K. Matsubayashi,¹ and J. B. Goodenough²

¹*Institute for Solid State Physics, University of Tokyo, Kashiwa 277-8581, Japan*

²*Texas Materials Institute, University of Texas at Austin, Austin, Texas 78712, USA*

(Received 23 October 2008; published 4 December 2008)

Measurements of dc conductivity and ac magnetic susceptibility under pressure to 12 GPa as well as of the crystal structure under pressure were made on antiferromagnetic LaMnO_3 and ferromagnetic $\text{LaMn}_{0.5}\text{Ga}_{0.5}\text{O}_3$ crystals. Collapse of magnetic ordering in both crystals has been found at a phase where the static Jahn-Teller distortion is suppressed. These results resolve the question whether a spin-ordered phase will survive if the orbital degree of freedom is released in an e orbital system, a topic of broad current interest.

DOI: [10.1103/PhysRevB.78.220402](https://doi.org/10.1103/PhysRevB.78.220402)

PACS number(s): 75.30.Et, 75.50.Ee, 62.50.-p

The colossal magnetoresistance effect and the multiferroic effect found in manganites revive the interest in orbital physics tracking back to the 1950s when the tie between spin ordering and the static orbital ordering had been worked out.¹ However, whether the intersite spin-spin interactions remain if orbitals keep fluctuating is still controversial. In order to tackle this problem, the $t_2^ne^0$ ($n=1,2$) systems of the orthorhombic perovskites LaTiO_3 and LaVO_3 have been studied intensively recently²⁻⁵ since they have the pseudocubic structure and the orbital-lattice interaction is relatively weak. In comparison with the $t_2^ne^0$ systems, the $t_2^3e^1$ system of LaMnO_3 has received almost no attention in this regard since the strong orbital-lattice interaction causes a cooperative Jahn-Teller (JT) ordering at 750 K (Ref. 6) and the type-A antiferromagnetic (AF) ordering sets in at 140 K.⁷ Strongly biased by an intrinsic structural distortion,⁸ the e orbitals are ordered alternately along a and b axes within the basal plane, which gives ferromagnetic coupling through the σ bonding $e^1\text{-O-}e^0$ competing with antiferromagnetic coupling via the π bonding $t^3\text{-O-}t^3$. It has been shown⁹ from the evolutions of T_N and the structural change as a function of the rare-earth ionic size that the JT distortion, instead of the orbital overlap integral, plays a dominant role in determining the strength of the $e^1\text{-O-}e^0$ interaction. Therefore, reducing the JT distortion under pressure appears to contribute to an anomalously large $d \ln T_N/dP$ found in LaMnO_3 at $P \leq 2.5$ GPa.¹⁰ As pressure increases further, the system undergoes two pressure-induced phase transitions; Raman spectra and a structural study under pressure suggest that orbital ordering collapses at $P \approx 18$ GPa and the transport data show a metal-insulator transition at 32 GPa.¹¹ These findings leave open the character of any magnetic interaction for the orbitally disordered insulator phase within $18 < P < 32$ GPa. The collapse of a cooperative JT (CJT) distortion at a pressure far below the critical pressure for the localized to itinerant electronic transition provides a chance for us to study whether the type-A magnetic order will give way to a ferromagnetic phase smoothly in the insulator phase in the absence of a static JT distortion. Moreover, as the metal-insulator transition is approached from the Mott insulator side, there is also a long-standing question whether the superexchange interaction evolves smoothly until the phase boundary. We have shown in the perovskite RNiO_3 that the perturbation formula of the superexchange interaction fails as the metal-insulator transition is approached.¹² By studying the magnetism in both type-A

antiferromagnetic LaMnO_3 and ferromagnetic $\text{LaMn}_{0.5}\text{Ga}_{0.5}\text{O}_3$ under hydrostatic pressure, we show that spin ordering does not survive when the e orbital ordering collapses in a Mott insulator.

Both perovskite crystals LaMnO_3 and $\text{LaMn}_{0.5}\text{Ga}_{0.5}\text{O}_3$ were grown with an infrared-heating image furnace and their thermoelectric power $\alpha > 600$ $\mu\text{V/K}$ means nearly perfect Mn^{3+} in both crystals. Pieces cut from the same ingots have been studied previously.^{10,13} The magnetic transition temperatures of these crystals match well with documented values. Pieces of these crystals were also pulverized into fine powder for x-ray diffraction (XRD) study under high pressure. The ac magnetic-susceptibility $\chi(T)$ measurements under pressure were carried out in a cubic module with sintered diamond anvils in a 250 ton press. The crystal bars of $0.3 \times 0.3 \times 0.7$ mm³ located inside a primary-secondary coil were placed inside a Teflon capsule 1.5 mm in diameter and 2.0 mm long filled with a mixture of Fluorinert F70 and F77 as the pressure medium. The XRD study under pressure was performed with a diamond-anvil cell mounted on a closed-cycle cryostat and a Rigaku x-ray generator having a fine focus rotating anode. Diffraction data were collected on an image plate and integrated as intensity versus 2θ by the software FIT2D. Lattice parameters were obtained through the d -value refinement with the software JADE. Profile refinement was made on the diffraction spectra under selected pressures with the software FULLPROF.

To detect antiferromagnetic ordering by using the primary-secondary-coil method is a challenging problem when the coils are located in a pressure cell with $P > 2$ GPa. The type-A spin ordering in the LaMnO_3 crystal creates a spikelike anomaly at T_N under $P < 2.5$ GPa as shown in Fig. 1(a), which is the same as reported in a previous high-pressure study.¹⁰ This anomalous peak broadens at higher pressures. As an indicator of T_N , the peak of $\chi(T)$ moves to higher temperatures as pressure increases. T_N versus P in this pressure range, shown in Fig. 1(d), tracks primarily the extension of the curve obtained at $P \leq 2$ GPa.¹⁰ However, the relative magnitude of the peak at T_N shown in Figs. 1(a) and 1(d) is no longer a constant. It reaches its maximum at about $P=8$ GPa, then decreases gradually as pressure increases further and falls into the noise level at the highest pressure in this work. An increase under pressure in the peak of $\chi(T)$ can be attributed to (a) the change in the coil-to-sample configuration and (b) a slight increase in the

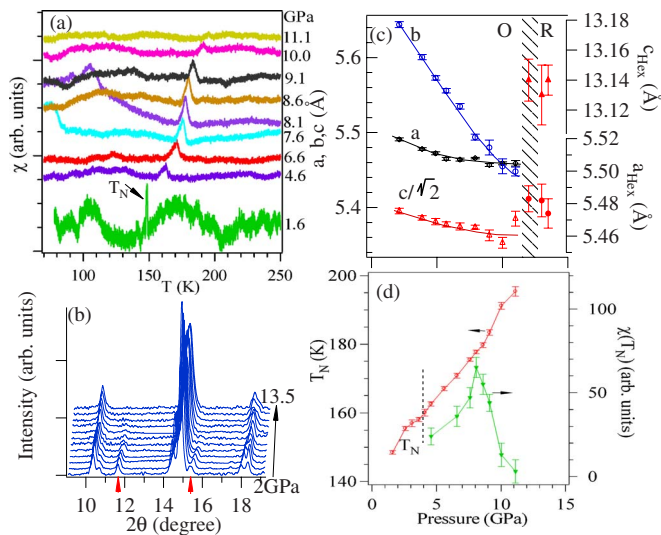


FIG. 1. (Color online) (a) The temperature dependence of ac (704 Hz) magnetic susceptibility $\chi(T)$ of LaMnO_3 under different pressures. (b) The x-ray powder diffraction of LaMnO_3 under different pressures. The peaks identified by small arrows are only allowed in the orthorhombic phase. (c) The pressure dependence of the lattice parameters of LaMnO_3 . Lines through data points are guides to the eyes. (d) The pressure dependence of Néel temperatures and the relative peak height at T_N of LaMnO_3 . Question mark at 11.2 GPa means that there is no clear magnetic signal above the noise level of the $\chi(T)$. Dashed lines stand for temperatures at which the XRD was made.

driving current in the primary coil as the wire resistance decreases under pressure. Neither of these factors can be used to account for the signal reduction at $P > 8$ GPa. The gradual reduction in magnetic signal at T_N and its final vanishing at $P \approx 11.4$ GPa may indicate a collapse of the magnetic phase. This pressure, however, is far below 18 GPa where the cooperative orbital ordering collapses as suggested from the previous report.¹¹ It is important here to address two critical issues before we elaborate further the implication of this finding: (a) whether the magnetic phase truly collapses at 11 GPa or the signal from the crystal falls below the sensitivity limit of the probe used and (b) whether there is a corresponding change in orbital ordering or a structural transition at 11 GPa. To this end, we turn to the structure study.

Neutron diffraction under pressure is ideal to reveal all possible local distortions and therefore the orbital ordering. Unfortunately, this work has not been carried out under $P > 8$ GPa.¹⁴ The assumption that the orbital ordering may collapse at $P_c = 18$ GPa was made based on the extension to higher pressure of the refinement of XRD under $P < 5$ GPa.¹¹ A thorough analysis of x-ray diffraction as a function of temperature and pressure in this work helps to clarify how the JT distortion evolves under pressure.

In orthorhombic LaMnO_3 with $Pbnm$ space group, the cooperative octahedral-site tilting around the b axis leads to the lattice parameter $b > a$. The orthorhombic strain factor $S \equiv 2(b-a)/(b+a)$ necessarily remains positive if $\text{MO}_{6/2}$ octahedra are rigid. Although XRD does not pick up magnetic superlattice peaks in the magnetically ordered phase, it can be useful for detecting the magnetic transition if the lattice

has corresponding changes on crossing T_N due to exchange striction. As reported from neutron diffraction at ambient pressure, the S factor of LaMnO_3 in Fig. 2(a) shows a broad maximum at T_N .¹⁵ We have used this relationship between magnetic ordering and the orthorhombic strain factor to determine to what pressure the type-A magnetic ordering persists. Figure 2(b) shows XRD data from LaMnO_3 at a temperature near T_N under two pressures. The structure of LaMnO_3 remains orthorhombic under 4.5 GPa, so that the splitting Δ between the (202) and (022) peaks is proportional to the S factor. Mapping out the peak splitting Δ versus temperature in Fig. 2(a) clearly shows a broad maximum at the temperature corresponding to T_N determined from magnetic susceptibility under the same pressure. In contrast, the XRD under 11.5 GPa shows a single peak in place of the (202) and (022) peaks for the phase at lower pressure. The peak width of this single peak exhibits no noticeable change with the best resolution of our high-pressure XRD in the temperature scan on crossing the possible T_N . One may wonder whether the type-A spin ordering converts to another AF phases at 11 GPa, so that the S factor no longer shows the same anomaly as seen in the type-A magnetic phase. In order to verify this possibility, we have investigated the resistivity under pressure. The temperature dependence of the derivative $d \ln \rho(T)/d(1/T)$, which generally shows an anomaly at the magnetic transition temperature, is featureless for LaMnO_3 under 12 GPa. Therefore, all our measurements under pressure of magnetic susceptibility, structural changes, and resistivity point to a collapse of magnetic ordering in LaMnO_3 under 11 GPa.

The most visible structural change in LaMnO_3 under pressure from XRD is that the (111) and (021) peaks of the $Pbnm$ phase in Fig. 1(b) lose strength gradually for $P > 8$ GPa and the S factor, Fig. 3, changes sign at about 9 GPa. As in other orthorhombic perovskite oxides,¹⁶ LaCrO_3 and LaGaO_3 , which will be discussed in more detail below, and SmNiO_3 (Ref. 17) under pressure, the vanishing of these two peaks and changing sign of the S factor are precursors of a first-order phase transition to the rhombohedral phase $R-3c$. The XRD data indicate a two-phase region near 11 GPa; the phase at $P > 12$ GPa can be refined with the rhombohedral structure. The pressure dependence of the room-temperature resistivity shows an anomaly near 10.5 GPa, which confirms a phase transition. The rhombohedral symmetry is incompatible with CJT distortion. As a matter of fact, the CJT does

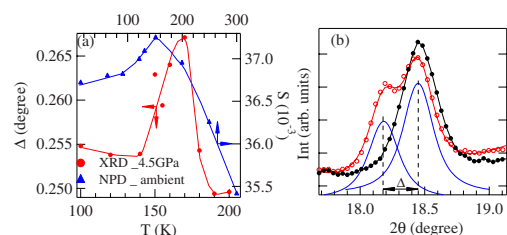


FIG. 2. (Color online) (a) Temperature dependence of the peak splitting between (202) and (022) peaks for LaMnO_3 at 4.5 GPa and S factor for the phase at ambient pressure (data for ambient pressure are from Ref. 15). (b) (202) and (022) peaks of XRD and their curve fitting from the orthorhombic LaMnO_3 ; circle symbol: 170 K at 4.5 GPa and solid symbol: 190 K at 11.5 GPa.

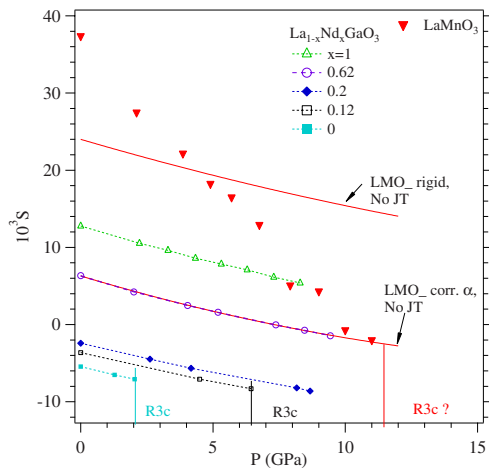


FIG. 3. (Color online) Pressure dependence of S factor for $\text{La}_{1-x}\text{Nd}_x\text{GaO}_3$ (data are from Ref. 18), LaMnO_3 , and $\text{LaMn}_{0.5}\text{Ga}_{0.5}\text{O}_3$.

not collapse abruptly at 11 GPa but gradually reduces even in the $Pbnm$ phase under pressure. The evolution of the CJT as a function of pressure can be derived from the pressure dependence of the S factor. A recent high-pressure study¹⁸ of $\text{La}_{1-x}\text{Nd}_x\text{GaO}_3$ provides the basis of how the orthorhombic perovskite structure responds to hydrostatic pressure since it has no mobile charge carriers or orbital degeneracy. More importantly, since the Nd substitution changes the geometric tolerance factor of the perovskite structure, the study includes the steric effect on the intrinsic orthorhombic distortion as well as the pressure effect. The $Pbnm$ space group can have $S=0$ if the octahedral-site tilting goes to zero, but it does not allow $S<0$ given rigid octahedra. With the software SPUDS,¹⁹ which is based on the bond-valence-sum rule and rigid octahedra, the structural simulation gives $S=18 \times 10^{-3}$ for LaGaO_3 whereas $S=-5.5 \times 10^{-3}$ has been observed in Fig. 3. The large difference between the calculated and observed S is due to a reduction from 90° of the O-M-O bond angle α subtending the b axis within an octahedral site.²⁰ This correction becomes smaller as the RMO_3 perovskite tolerance factor $t \equiv (R-O)/\sqrt{2}(M-O)$ decreases. The increase in S as R changes from La to Nd shown in Fig. 3 reflects a combination of a reduced α angle correction and an increased orthorhombic distortion. From Fig. 3, it is clear that pressure turns S from a positive value toward a negative value or enlarges a negative S in the whole series $\text{La}_{1-x}\text{Nd}_x\text{GaO}_3$. It is important to note that the pressure dependences of S for all members of the system $\text{La}_{1-x}\text{Nd}_x\text{GaO}_3$ are nearly identical. Since $S<0$ is not allowed in the $Pbnm$ structure with rigid octahedra, the pressure effect on these insulators, which does not depend on the t factor, is primarily to reduce the angle α . However, the magnitude of the α correction to S depends on the t factor. Now we turn to orthorhombic LaMnO_3 . The calculation with SPUDS gives $S=24 \times 10^{-3}$ for the rigid LaMnO_3 lattice without a JT distortion. The correction due to $\alpha<90^\circ$ makes S of this compound happen to be nearly the same as that of $\text{La}_{0.38}\text{Nd}_{0.62}\text{GaO}_3$. The pressure dependence of S for LaMnO_3 without a JT distortion was obtained as follows: we first fit S versus P of $\text{La}_{1-x}\text{Nd}_x\text{GaO}_3$ with a polynomial formula and then scaled it

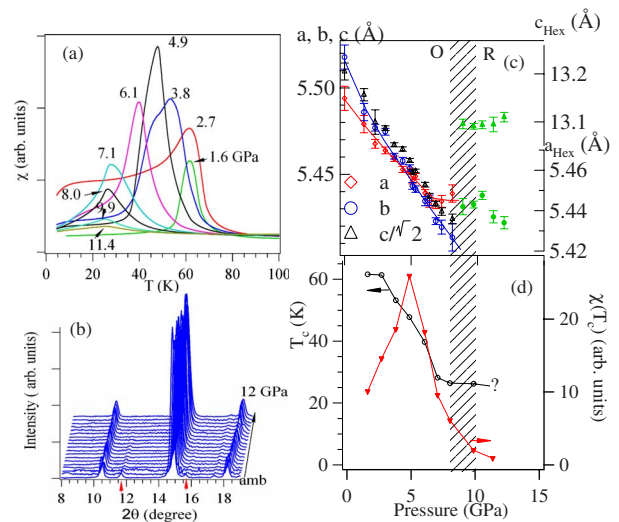


FIG. 4. (Color online) The same as Fig. 1 for $\text{LaMn}_{0.5}\text{Ga}_{0.5}\text{O}_3$.

by S_0 of LaMnO_3 without a JT distortion at ambient pressure. For a reason which is still unclear, the JT distortion enhances S of LaMnO_3 significantly as is shown by data points in Fig. 3, and pressure reduces S in a much steeper slope than that by just enlarging the α correction. At the same pressure where the observed S approaches the line expected for LaMnO_3 without a JT distortion, the magnetically ordered phase collapses.

Ga^{3+} substitution in $\text{LaMn}_{1-x}\text{Ga}_x\text{O}_3$ converts the type-A antiferromagnetic order in LaMnO_3 into ferromagnetic order for compositions $0.5 \leq x \leq 0.6$.^{13,21} An orbital ordering with a mixture of two e orbitals has been proven to be the origin of the ferromagnetic interaction in the orthorhombic $\text{LaMn}_{1-x}\text{Ga}_x\text{O}_3$.²² The same measurements as in Fig. 1 for antiferromagnetic LaMnO_3 have been carried out on the ferromagnetic $\text{LaMn}_{0.5}\text{Ga}_{0.5}\text{O}_3$ in Fig. 4. Like most ferromagnets, Fig. 4(a) shows that pressure suppresses T_c in $\text{LaMn}_{0.5}\text{Ga}_{0.5}\text{O}_3$. The peak height of $\chi(T)$ at T_c in Fig. 4(d) increases at lower pressures and vanishes at the phase boundary of the orthorhombic to rhombohedral phase transition in exactly the same way as in AF LaMnO_3 . However, the structural transition to the rhombohedral phase in Figs. 4(b) and 4(c) occurs at a relatively lower pressure since the compound has a smaller orthorhombic distortion at ambient pressure. A very clean, strong signal of the ac susceptibility in Fig. 4(a) leaves no doubt that the ferromagnetic ordering in $\text{LaMn}_{0.5}\text{Ga}_{0.5}\text{O}_3$ is suppressed at $P>10$ GPa. A recent high-pressure study²³ of $\text{LaMn}_{1-x}\text{Ga}_x\text{O}_3$ with synchrotron radiation shows a transition at 9 GPa to the phase with higher symmetry in compositions with low Ga doping and confirmed the transition to $R-3c$ at 8 GPa for the composition $x \approx 0.5$.

One may argue that the type-A antiferromagnetic ordering in the orthorhombic phase of LaMnO_3 is suppressed by a competition between an antiferromagnetic interaction through t -O- t coupling and a ferromagnetic interaction through the e -O- e coupling that is greatly enhanced in the rhombohedral phase. This scenario, however, fails to explain why the ferromagnetism in the orthorhombic

LaMn_{0.5}Ga_{0.5}O₃ phase also collapses at the O-R phase boundary if the ferromagnetic interaction is enhanced in the R-3c phase. We are left with the solution that superexchange interactions in an orbitally degenerate *e* orbital system do not give a spin-ordered state.

Opening an orbital degree of freedom in a Mott insulator introduces a dynamics to the spin-orbital system where superexchange interactions would mediate any possible spin and even orbital orderings. Theoretical solutions derived from the Hamiltonian²⁴ postulated by Kugel and Khomskii (KK) include quantum melting of magnetic ordering in the *e* orbital system,²⁵ magnetic ordering prohibited by symmetry in the KK Hamiltonian,²⁶ spin-orbital entanglement,²⁷ and a spontaneous orbital/spin ordering through the order-from-disorder scenario.^{28,29} In transition-metal oxides, the orbital-lattice interaction lifts an orbital degeneracy at high temperatures by the CJT distortion, which may be biased by an intrinsic structural distortion. However, the CJT distortion is avoided where (a) there is a relatively weak orbital-lattice interaction in the cubic crystal field or (b) the crystal structure has a single metal-oxygen bond length allowed by the structural symmetry. The first case is nearly fulfilled in the $t_2^ne^0$ ($n=1,2$) systems of the orthorhombic perovskites LaTiO₃ and LaVO₃, whereas the orbital degree of freedom in the *e* orbital system can be released through procedure (b). The rhombohedral symmetry is not compatible with orbital orderings so that an orbital degeneracy remains to lowest temperature. Alternatively, the frustrated superexchange interaction can also be from an orbital-glass phase which

should not take the feedback of spin-spin interaction in a joint spin/orbital space. However, an orbital-glass phase is unlikely for LaMnO₃ under 12 GPa since it would prefer the cubic symmetry. It is interesting to test whether a sufficiently high magnetic field will induce a magnetically ordered state in rhombohedral LaMnO₃ where the orbital ordering, if it exists, would be caused by a superexchange interaction alone. Although it has been actively discussed in recent years,^{25,30} the new physics due to an entanglement of spin and orbital degrees of freedom in an *e* orbital system remains to be explored further experimentally.

In conclusion, both type-A antiferromagnetic order in LaMnO₃ and ferromagnetic order in LaMn_{0.5}Ga_{0.5}O₃ survive under high pressure as long as the cooperative Jahn-Teller distortion remains. The opposite pressure dependence of the magnetic transition temperatures in these two compounds reflects a sharp difference in the exchange striction at the magnetic transition. Signals of the magnetic susceptibility at both T_c and T_N vanish under pressure at a transition to the rhombohedral R-3c structure, which is incompatible with a cooperative JT distortion. We have shown experimentally that the orbital degree of freedom can be released in an *e* orbital system while it remains a Mott insulator and that intersite spin-orbital entanglement that results does not lead to a spin-ordered phase.

This work is supported by NSF in USA and KAKENHI in Japan.

*jszhou@mail.utexas.edu

- ¹J. B. Goodenough, *Phys. Rev.* **100**, 564 (1955).
- ²G. Khaliullin and S. Maekawa, *Phys. Rev. Lett.* **85**, 3950 (2000).
- ³B. Keimer, D. Casa, A. Ivanov, J. W. Lynn, M. v. Zimmermann, J. P. Hill, D. Gibbs, Y. Taguchi, and Y. Tokura, *Phys. Rev. Lett.* **85**, 3946 (2000).
- ⁴S. Miyasaka, J. Fujioka, M. Iwama, Y. Okimoto, and Y. Tokura, *Phys. Rev. B* **73**, 224436 (2006).
- ⁵G. Khaliullin, P. Horsch, and A. M. Oles, *Phys. Rev. Lett.* **86**, 3879 (2001).
- ⁶J. Rodriguez-Carvajal *et al.*, *Phys. Rev. B* **57**, R3189 (1998).
- ⁷F. Moussa, M. Hennion, J. Rodriguez-Carvajal, H. Moudou, L. Pinsard, and A. Revcolevschi, *Phys. Rev. B* **54**, 15149 (1996).
- ⁸J.-S. Zhou and J. B. Goodenough, *Phys. Rev. B* **77**, 132104 (2008).
- ⁹J.-S. Zhou and J. B. Goodenough, *Phys. Rev. Lett.* **96**, 247202 (2006).
- ¹⁰J.-S. Zhou and J. B. Goodenough, *Phys. Rev. Lett.* **89**, 087201 (2002).
- ¹¹I. Loa, P. Adler, A. Grzechnik, K. Syassen, U. Schwarz, M. Hanfland, G. Kh. Rozenberg, P. Gorodetsky, and M. P. Pasternak, *Phys. Rev. Lett.* **87**, 125501 (2001).
- ¹²J.-S. Zhou, J. B. Goodenough, and B. Dabrowski, *Phys. Rev. Lett.* **95**, 127204 (2005).
- ¹³J.-S. Zhou, H. Q. Yin, and J. B. Goodenough, *Phys. Rev. B* **63**, 184423 (2001).
- ¹⁴L. Pinsard-Gaudart, J. Rodriguez-Carvajal, A. Daoud-Aladine, I. Goncharenko, M. Medarde, R. I. Smith, and A. Revcolevschi, *Phys. Rev. B* **64**, 064426 (2001).
- ¹⁵Q. Huang, A. Santoro, J. W. Lynn, R. W. Erwin, and J. A. Borchers, *Phys. Rev. B* **55**, 14987 (1997).
- ¹⁶T. Shibusaki, T. Furuya, J. Kuwahara, Y. Takahashi, H. Takahashi, and T. Hashimoto, *J. Therm. Anal. Calorim.* **81**, 575 (2005).
- ¹⁷M. Amboage, M. Hanfland, J. A. Alonso, and M. J. Martinez-Lope, *J. Phys.: Condens. Matter* **17**, S783 (2005).
- ¹⁸R. J. Angel, J. Zhao, N. L. Ross, C. V. Jakeways, S. A. T. Redfern, and M. Berkowski, *J. Solid State Chem.* **180**, 3408 (2007).
- ¹⁹M. W. Lufaso and P. M. Woodward, *Acta Crystallogr., Sect. B: Struct. Sci.* **57**, 725 (2001).
- ²⁰J.-S. Zhou and J. B. Goodenough, *Phys. Rev. Lett.* **94**, 065501 (2005).
- ²¹J. Blasco, J. Garcia, J. Campo, M. C. Sanchez, and G. Subias, *Phys. Rev. B* **66**, 174431 (2002).
- ²²J.-S. Zhou and J. B. Goodenough, *Phys. Rev. B* **77**, 172409 (2008).
- ²³M. Baldini, L. Malavasi, D. D. Castro, A. Nucara, W. Crichton, M. Mezouar, J. Blasco, and P. Postorino, arXiv:0807.2848 (unpublished).
- ²⁴K. I. Kugel and D. I. Khomskii, *Sov. Phys. Usp.* **25**, 231 (1982).
- ²⁵L. F. Feiner, A. M. Oles, and J. Zaanen, *Phys. Rev. Lett.* **78**, 2799 (1997).
- ²⁶A. B. Harris, T. Yildirim, A. Aharony, O. Entin-Wohlman, and I. Ya. Korenblit, *Phys. Rev. Lett.* **91**, 087206 (2003).
- ²⁷A. M. Oleś, P. Horsch, L. F. Feiner, and G. Khaliullin, *Phys. Rev. Lett.* **96**, 147205 (2006).
- ²⁸G. Khaliullin and V. Oudovenko, *Phys. Rev. B* **56**, R14243 (1997).
- ²⁹G. Khaliullin, *Phys. Rev. B* **64**, 212405 (2001).
- ³⁰L. F. Feiner and A. M. Oles, *Phys. Rev. B* **59**, 3295 (1999).